Supplementary Materials for

Combating the SARS-CoV-2 Omicron (BA.1) and BA.2 with potent bispecific antibodies engineered from non-Omicron neutralizing antibodies

Yingdan Wang[1#], Xiang Zhang[1#], Yunping Ma[1,2#], Yanqun Wang[3#], Wuqiang Zhan[1], Qinwen Zheng[1], Meng Zhang[1], Ping Ji[1], Mei Liu[1], Qianying Liu[1], Tingting Sun[1], Tongyu Zhu[1], Yumei Wen[1], Lei Sun[1]*, Jincun Zhao[3,4,5]*, Fan Wu[2]*, Zhenguo Chen[1]*, Jinghe Huang[1]*

[1]Key Laboratory of Medical Molecular Virology (MOE/NHC/CAMS) and Shanghai Institute of Infectious Disease and Biosecurity, the Fifth People's Hospital of Shanghai, Shanghai Public Health Clinical Center, Institutes of Biomedical Sciences, School of Basic Medical Sciences, Fudan University, Shanghai, China.

[2]Shanghai Immune Therapy Institute, Shanghai Jiao Tong University School of Medicine Affiliated Renji Hospital, Shanghai, China.

[3]State Key Laboratory of Respiratory Disease, National Clinical Research Center for Respiratory Disease, Guangzhou Institute of Respiratory Health, the First Affiliated Hospital of Guangzhou Medical University, Guangzhou, Guangdong, China;

[4]Institute of Infectious Disease, Guangzhou Eighth People's Hospital of Guangzhou Medical University, Guangzhou, Guangdong, China.

[5]Guangzhou Laboratory, Bio-island, Guangzhou 510320, China

[#]These authors contributed equally.
*Correspondence to: llsun@fudan.edu.cn, zhaojincun@gird.cn, wufan@renji.com, ZhenguoChen@fudan.edu.cn, or jinghehuang@fudan.edu.cn.

Table S1. Mutations in spike proteins of Omicron, BA.1.1, BA.2 and BA.3.

Spkie		Muation	BA.1	BA.1.1	BA.2	BA.3
NTD		T19I			■	
		Δ24-26			■	
		A27S			■	
		A67V	■	■		■
		Δ69-70	■	■		■
		T95I	■	■		■
		G142D	■	■	■	■
		Δ143-145	■	■		■
		Δ211	■	■		■
		L212I	■	■		■
		V213G			■	
		ins214EPE	■	■		
RBD		G339D	■	■	■	■
		R346K		■		
		S371L/F	L	L	F	F
		S373P	■	■	■	■
		S375F	■	■	■	■
		T376A			■	
		D405N			■	■
		R408S			■	
	RBM	K417N	■	■	■	■
		N440K	■	■	■	■
		G446S	■	■		■
		S477N	■	■	■	■
		T478K	■	■	■	■
		E484A	■	■	■	■
		Q493R	■	■	■	■
		G496S	■	■		
		Q498R	■	■	■	■
		N501Y	■	■	■	■
		Y505H	■	■	■	■
SD1		T547K	■	■		
SD2		D614G	■	■	■	■
		H655Y	■	■	■	■
		N679K	■	■	■	■
		P681H	■	■	■	■
FP		N764K	■	■	■	■
		D796Y	■	■	■	■
		N856K	■	■		
HR1		Q954H	■	■	■	■
		N969K	■	■	■	■
		L981F	■	■		

40 **Table S2. The germline and CDRH3 sequences of GW01, 4L12, and 16L9.**

Donor ID	mAb ID	VH	CDRH3 sequence	VL	CDRL3 sequence
Donor 1	GW01	IGHV3-43	AKDRSYGPPDVFNYEYGMDV	IGLV1-44	AAWDDSLNWV
Donor 1	4L12	IGHV3-66	ARDLITYGMDV	IGKV1-9	QQLNSYPPLT
Donor 2	16L9	IGHV3-53	ARGEIQPYYYYGMDV	IGLV2-8	SSYAGSSNFDV

41

**Table S3. Cryo-EM data collection and refinement statistics of SARS-CoV-2 complexed with IgG FD01.**

	State 1	State 2	State 3	State 4	State 5	State 6	Local refine NRF
Data collection and processing							
Magnification				81,000			
Voltage (kV)				300			
Electron exposure (e–/Å^2)				58			
Defocus range (μm)				-1.2 to -2.5			
Pixel size (Å)				1.064			
Initial particles (no.)				1,003,956			
Symmetry imposed				C1			
Final particles (no.)	194,026	62,040	74,415	141,577	39,294	71,568	249,122
Map resolution (Å)	3.47	3.70	3.91	3.47	3.87	6.11	3.51
Refinement							
R.m.s. deviations							
Bond lengths (Å)	0.003	0.003	0.003	0.003	0.003	0.002	0.002
Bond angles (°)	0.539	0.506	0.499	0.557	0.527	0.437	0.524
Validation							
MolProbity score	2.52	2.48	2.46	2.50	2.53	2.41	2.88
Clashscore	9.18	8.06	8.38	8.44	8.14	7.67	10.97
Rotamer outlier (%)	5.14	5.34	5.30	5.39	5.97	5.33	9.21
Ramachandran plot							
Favored (%)	91.75	92.00	92.74	91.84	91.67	93.20	88.62
Allowed (%)	7.95	7.90	7.14	8.13	8.17	6.80	11.38
Disallowed (%)	0.30	0.11	0.13	0.03	0.16	0.00	0.00
EMDB	32655	32656	32657	32659	32660	32661	32654
PDB	7WOQ	7WOR	7WOS	7WOU	7WOV	7WOW	7WOP

45
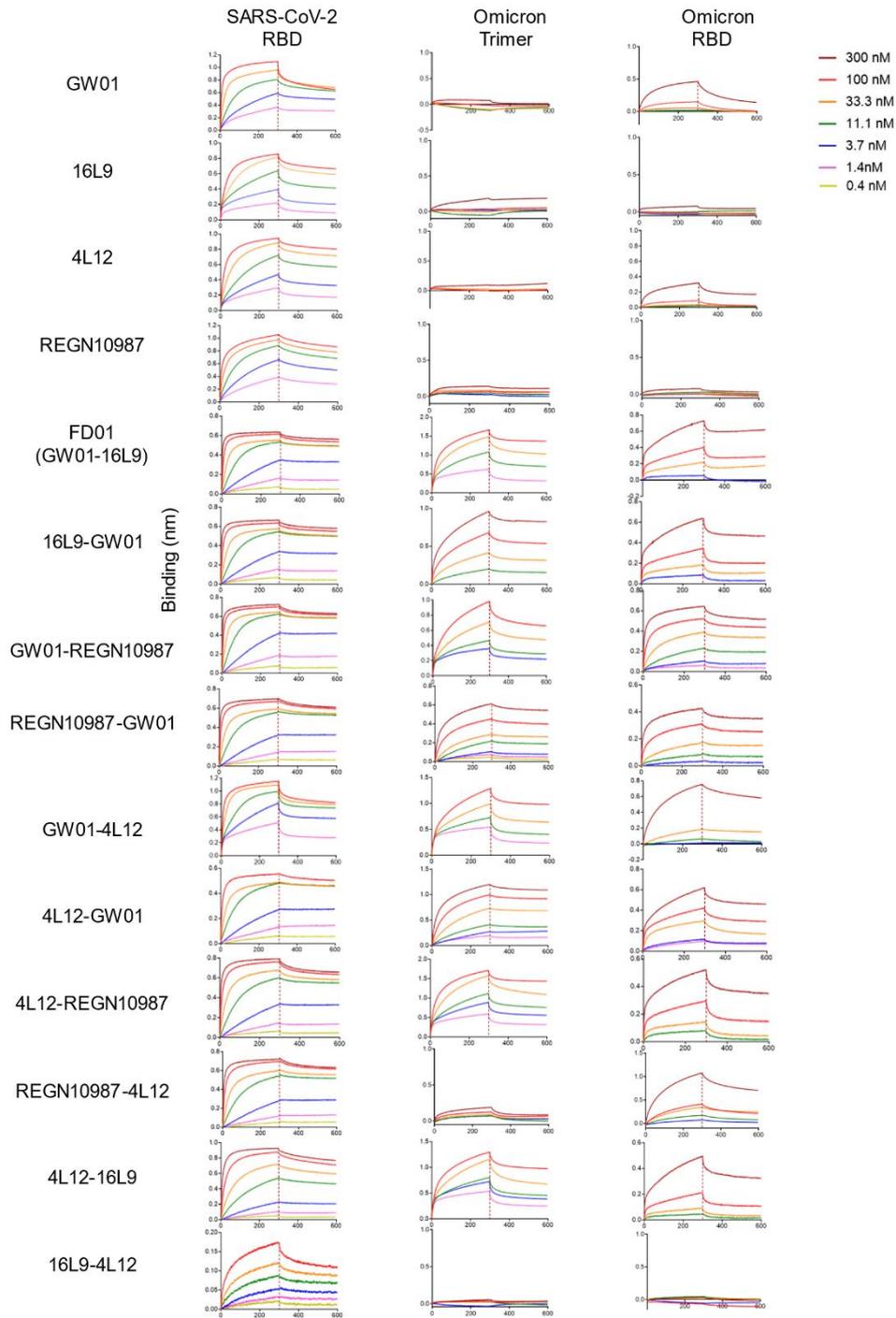
Fig. S1. Binding affinities of GW01, 16L9, 4L12, REGN10987, and ten bispecific antibodies to SARS-CoV-2 RBD-his, Omicron trimer-his and Omicron RBD-his measured by bilayer interferometry. Antibodies were immobilized on anti-human IgG (AHC) biosensors and then tested for their binding abilities to the target proteins.

46

47

48

49

50

a

b

c

Omicron S-FD01

State 1
State 2
State 3
State 4
State 5

3.87 Å   3.47 Å   3.47 Å
3.91 Å   3.70 Å

Omicron S-FD01

State 6

6.11 Å

d

16L9

GW01

e

GSFSC Resolution: 3.51Å

No Mask (4.3Å)
Spherical (3.9Å)
Tight (3.5Å)
Corrected (3.5Å)

f

R493

RBD AA[490-499]

T376
F377   F374

RBD AA[373-380]

Y230
Y229

16L9 AA[229-237]

N233
Y234   Y232   Y226

GW01 AA[226-234]
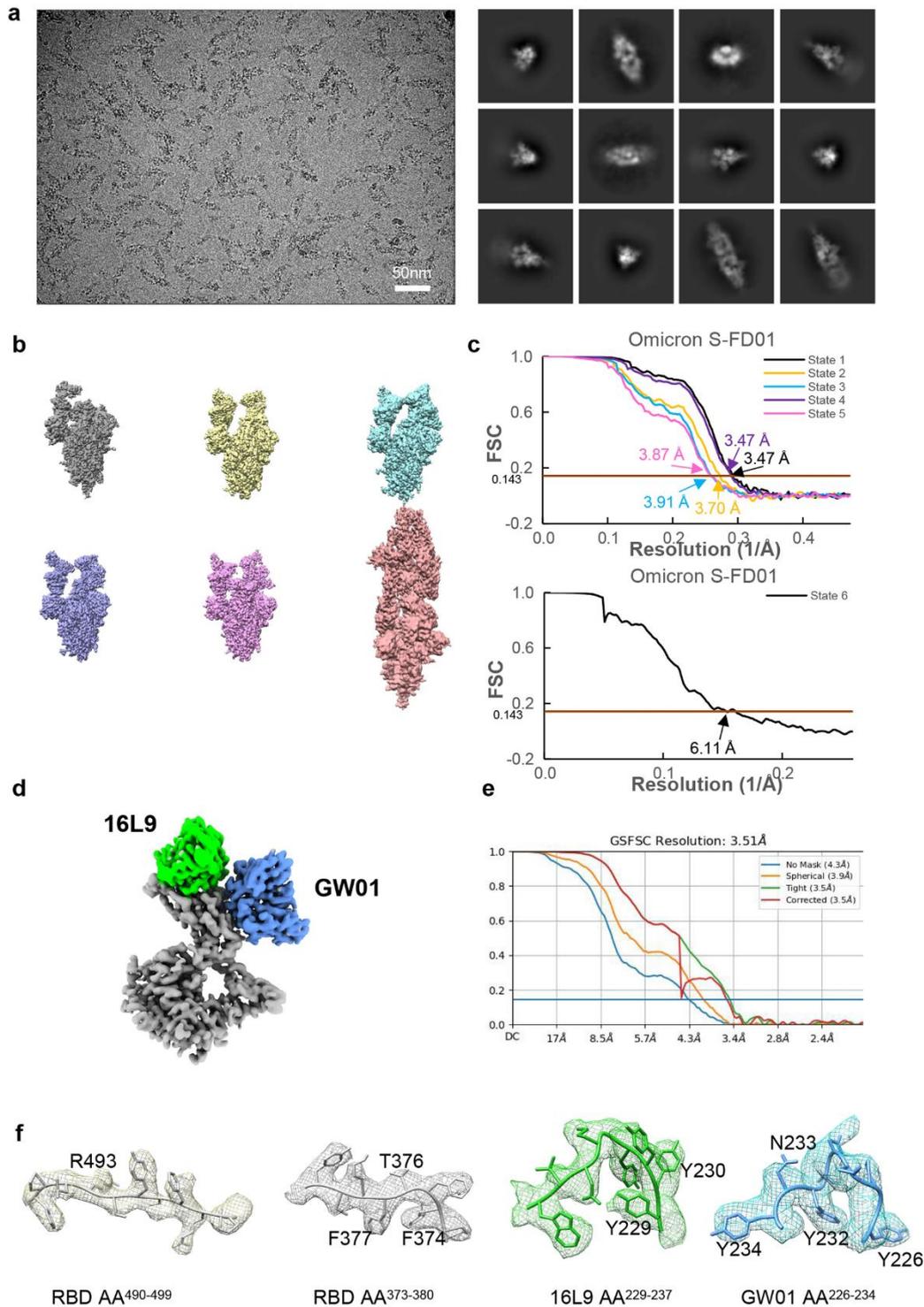
51

52

53 **Fig. S2. Cryo-EM data collection and processing of FD01 bound SARS-CoV-2**

54 **Omicron S. (a)** Representative electron micrograph and 2D classification results of

55 FD01 bound SARS-CoV-2 S. **(b)** The reconstruction map of the complex structures at

56 six states. **(c)** Gold-standard Fourier shell correlation curves generated in RELION for

57 structures of six states. The 0.143 cut-off is indicated by a horizontal dashed line. **(d)**

58 The local-refined map of the NRF region. **(e)** Gold-standard Fourier shell correlation

59 curves generated in cryoSPARC for local-refined map. (**f**) Density maps of residues

60 around the interface.

61
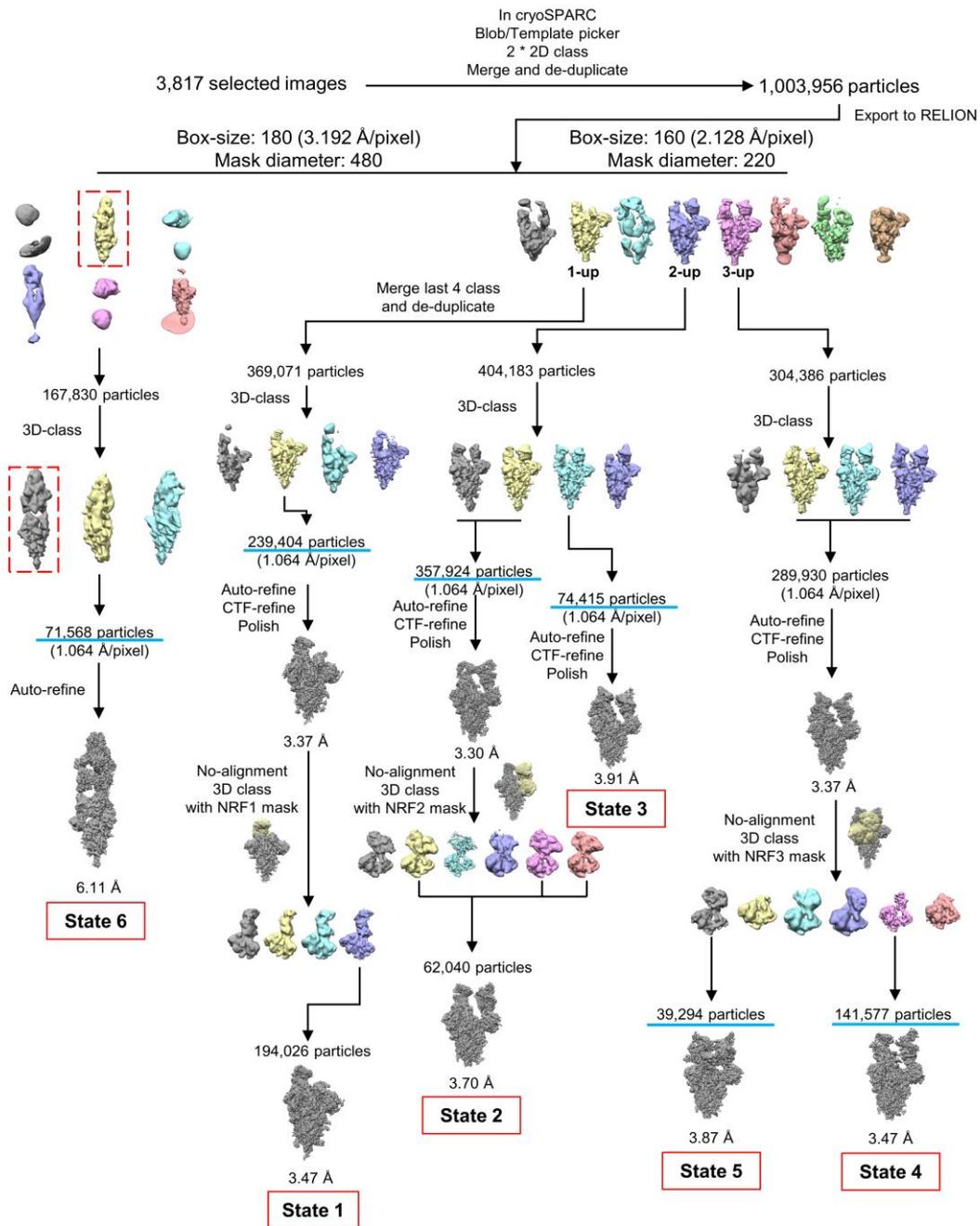
Fig. S3. Data processing flowchart of FD01 bound SARS-CoV-2 Omicron S trimer. Particles number above cyan line is used for particle counting statistics.

Select all 3D-classes of OS-trimer
with good RBD and FD01 density
De-duplicate

217,667 particles
(1.064 Å/pixel)

Auto-refine with reference
aligned C3 symmetry

Expand particles with C3 symmetry
653,001 particles

Subtract with one NRF mask
No-alignment 3D class

249,122 particles

Export to cryoSPARC
Local refinement

3.51 Å

64
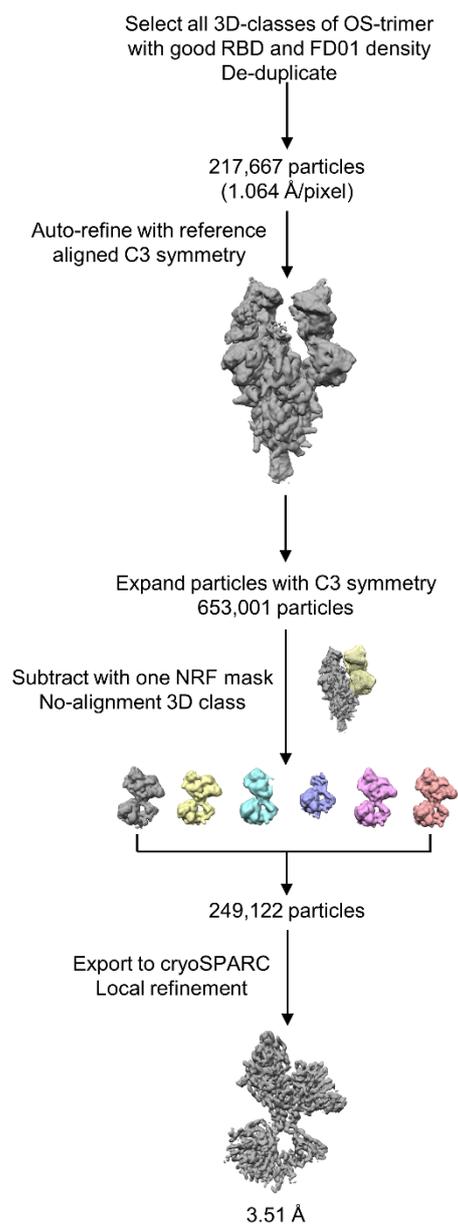
Fig. S4. Data processing flowchart of local refinement of RBD-FD01.

65

66
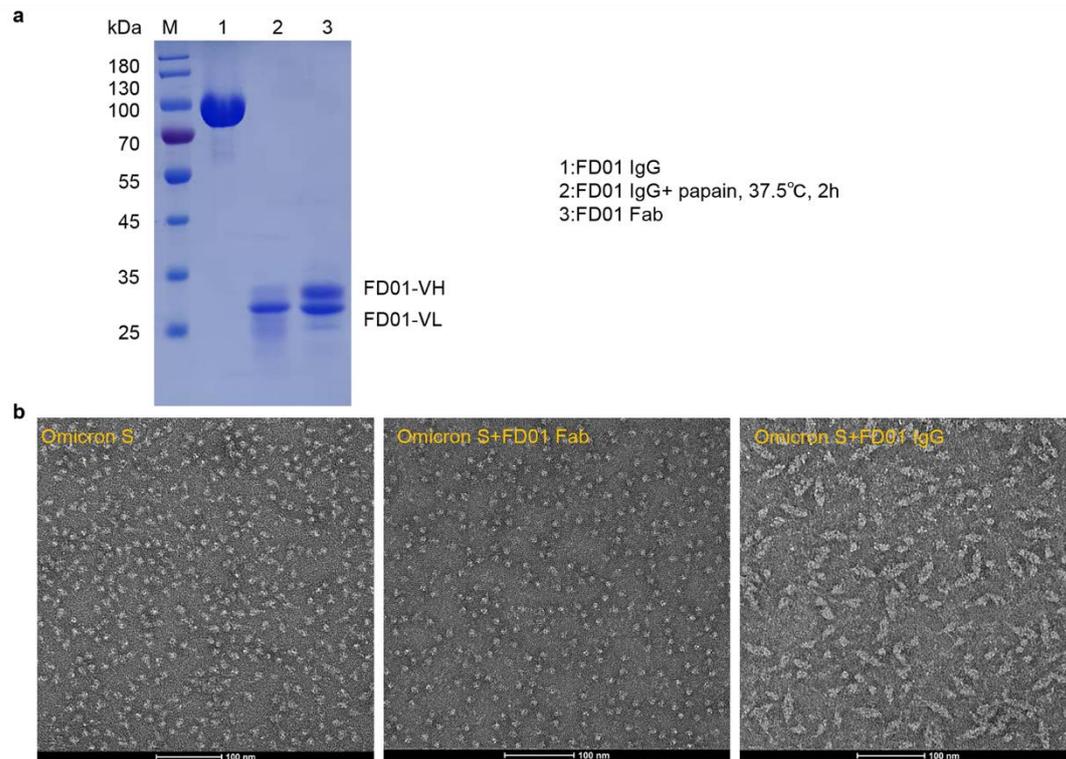
67 **Fig. S5. IgG FD01 crosslinks Omicron S trimers to form trimer dimer**

68 **conformation.** (**a**) SDS-PAGE of the FD01 in IgG and Fab form; (**b**) Negative stain

69 images of Omicron S trimer-FD01 Fab and Omicron S trimer-FD01 IgG, showing that

70 only IgG FD01 can induce the formation of trimer dimer.

71
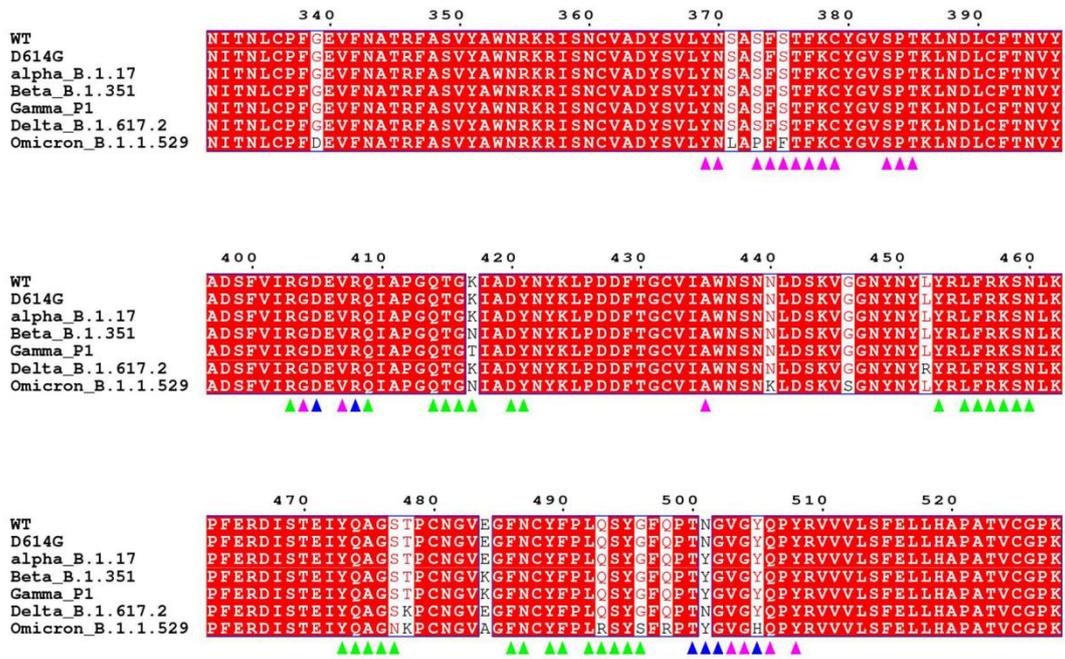
Fig. S6. Sequence alignment of SARS-CoV-2 WT and all VOCs RBDs. Conserved amino acids are highlighted as red. Residues involved in 16L9 or GW01 are marked with triangles in green or magenta, respectively. Residues involved in both 16L9 and GW01 binding are marked with triangles in blue.

97
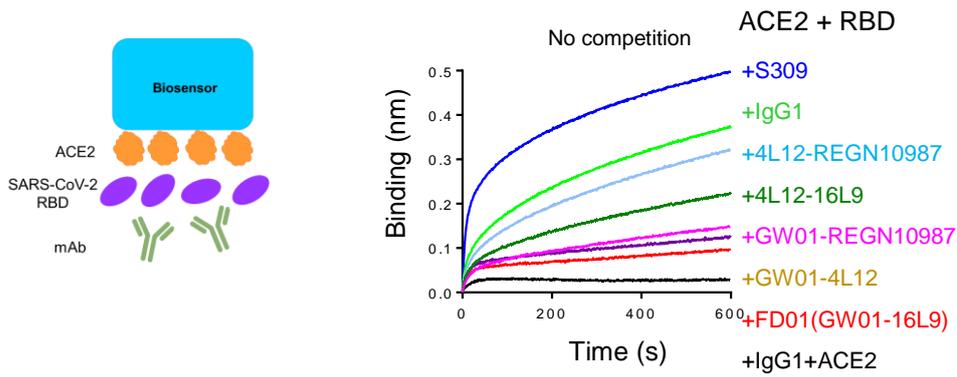
98
99
100 **Fig. S7. Five representative bispecific antibodies block RBD binding to ACE2.**

101 Binding of ACE2 to the SARS-CoV-2 RBD in competition with bispecific antibodies

102 (red), S309 (blue), control IgG1 (green), and IgG1+ACE2 (black).

103

104
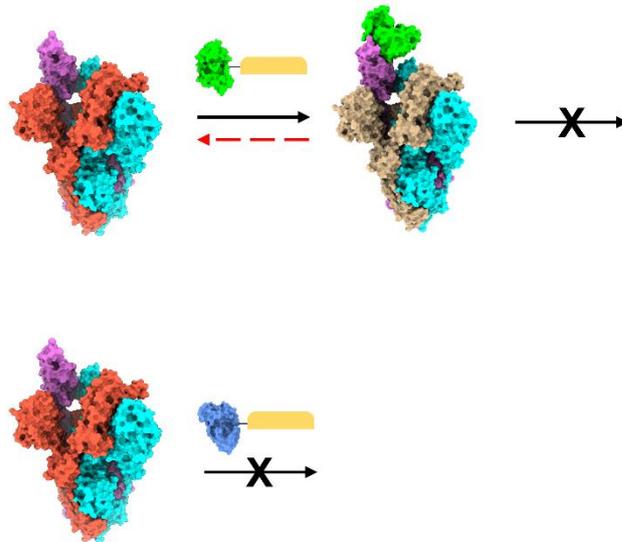
Fig. S8. Hypothesis of binding features when Omicron S trimer meets with mAbs of 16L9 or GW01.

107
108
109
110
111
112
113
114
115
116
117
118
119
120
121
122
123
124
125
126
127
128
129
130
131

132   **Supplementary Video: Conformation transitions of Omicron S trimer and the**
133   **representative bispecific antibody GW01-16L9 (FD01) in six states.**